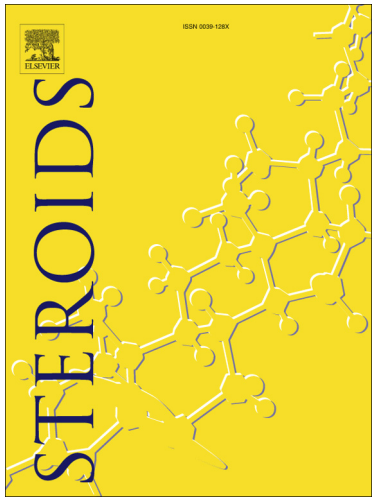

Conjugates of 17-substituted testosterone and epitestosterone with pyropheophorbide a differing in the length of linkers

Vladimir A. Zolottsev, Gelii V. Ponomarev, Maria O. Taratynova, Galina E. Morozevich, Roman A. Novikov, Vladimir P. Timofeev, Pavel N. Solyev, Maria G. Zavialova, Olga V. Zazulina, Yaroslav V. Tkachev, Alexander Y. Misharin

PII: S0039-128X(18)30121-1
DOI: https://doi.org/10.1016/j.steroids.2018.06.011
Reference: STE 8282

To appear in: *Steroids*

Received Date: 12 February 2018
Revised Date: 5 June 2018
Accepted Date: 8 June 2018

Please cite this article as: Zolottsev, V.A., Ponomarev, G.V., Taratynova, M.O., Morozevich, G.E., Novikov, R.A., Timofeev, V.P., Solyev, P.N., Zavialova, M.G., Zazulina, O.V., Tkachev, Y.V., Misharin, A.Y., Conjugates of 17-substituted testosterone and epitestosterone with pyropheophorbide a differing in the length of linkers, *Steroids* (2018), doi: https://doi.org/10.1016/j.steroids.2018.06.011

CONJUGATES OF 17-SUBSTITUTED TESTOSTERONE AND EPITESTOSTERONE WITH PYROPHEOPHORBIDE a DIFFERING IN THE LENGTH OF LINKERS.

Vladimir A. ZOLOTTSEV[1], Gelii V. PONOMAREV[1], Maria O. TARATYNOVA[1], Galina E. MOROZEVICH[1] , Roman A. NOVIKOV[2], Vladimir P. TIMOFEEV[2], Pavel N. SOLYEV[2], Maria G. ZAVIALOVA[1], Olga V. ZAZULINA[1], Yaroslav V. TKACHEV[2], Alexander Y. MISHARIN[1]

[1]Orekhovich Institute of Biomedical Chemistry, Moscow, Russia

[2]Engelhardt Institute of Molecular Biology RAS, Moscow, Russia

Keywords:

steroid conjugates; chemical synthesis; tetrapyrrolic macrocycles; molecular models; interaction with prostate carcinoma cells; structure-activity relationships.

Highlights:

- Testosterone and epitestosterone chemically conjugated with pyropheophorbide a
- Spectral properties and molecular models of conjugates are presented
- Epitestosterone conjugates inhibit LNCaP and PC-3 cells growth stronger
- Conformationally rigid conjugates possess stronger anti-proliferative activity

Abstract

Conjugates of 17α-substituted testosterone (**1** and **2**) and 17β-substituted epitestosterone (**3** and **4**) with pyropheophorbide a were synthesized. The scheme consisted of synthesis of 17α-hydroxy-3-oxopregn-4-en-21-oic and 17β-hydroxy-3-oxopregn-4-en-21-oic acids, and their coupling with pyropheophorbide a by means of either ethylene diamine, or 1,5-diamino pentane linkers. Mutual influence of steroidal and macrocyclic fragments in conjugates molecules was dependent on configuration of C17 and length of linker, that was established by analysis of ^{1}H NMR spectra and molecular models of conjugates. Studies of interaction of conjugates with prostate carcinoma cells revealed that their uptake and internalization were independent on the androgen receptor activity, but dependent on the structure of conjugates, decreasing in the following row: **3 > 4 ≥ 1 > 2**. Conjugates significantly decreased the LNCaP and PC-3 cells growth at 96 h incubation. Epitestosterone derivatives **3** and **4** also showed superior anti-proliferative activity *versus* testosterone ones. Conformationally more rigid conjugates **1** and **3**, comprising short linkers, were more active than those with long linkers; conjugate **3** was the most potent.

1. INTRODUCTION

Conjugation of steroids with some biologically active molecules, particularly with anticancer agents, is a prospective approach to develop new bifunctional constructs possessing enhanced efficiency and delivery to specific targets. The inclusion of steroid residues in the molecular structure of conjugates could ascribe them with new physicochemical and biological properties, as well as new morphological features related to self-assembly [1-9]. Steroid conjugates containing metallo-drugs, DNA alkylating agents, some specific peptides, peptidomimetics and peptoids have been synthesized and used for targeting androgen receptor [review 10, and the ref. therein].

Pyropheophorbide a derivatives are widely used as sensitizers for photodynamic therapy (PDT) of tumors. Particularly, amides of pyropheophorbide a efficiently decreased Eca 109 tumor in nude mice after irradiation [11]; triphenylphosphonium-pyropheophorbide a conjugates had affinity to mitochondria, stimulate apoptosis, and boosted the cytotoxicity in 4T1 cells [12]; conjugation of pyropheophorbide a with cyclic RGD peptide significantly improved the tumor enrichment and tumor selectivity of pyropheophorbide a, as well as abolished the xenograft tumors in the murine model through one-time PDT treatment [13]; pyropheophorbide a methyl ester and PDT enhanced effect of HSV1-TK/GCV gene therapy on prostate cancer [14].

Conjugates of steroids, oxysterols, and bile acids with tetrapyrrolic macrocycles also have wide range of biomedical applications such as optical imaging, fluorescent labeling and photodynamic therapy [15-17]. Estradiol based pyropheophorbide a conjugate efficiently internalized by estrogen receptor positive cells, accumulated in nuclei, and revealed a potency of application as sensitizer for photodynamic therapy of breast cancer [18]. Recently reported testosterone based pyropheophorbide a conjugate **1** (Figure 1) exhibited antiproliferative activity and photoinduced cytotoxicity in prostate carcinoma cells [19].

In the present study we have synthesized new testosterone-pyropheophorbide a conjugate **2**, comprising 1,5-diaminopentane instead of ethylene diamine linker, as well as related epitestosterone-pyropheophorbide a conjugates **3** and **4** (Figure 1). We were interested in question how structural peculiarities of conjugates such as configuration of C17 and length of linker affect their conformation and biological activity. We investigated spectral properties and molecular models of conjugates **1 – 4**, and compared their interaction with cultured prostate carcinoma cells. The data presented herein revealed that uptake and internalization of conjugates by LNCaP prostate carcinoma cells, as well as potency to inhibit LNCaP and PC-3 cells growth were dependent on their structure.

2. EXPERIMENTAL

2.1. MATERIALS AND GENERAL METHODS

HRMS were registered on a Bruker 'Apex Ultra' FT ICR MS and a Bruker 'Daltonics micrOTOF-Q II' instruments at ion positive electro spray ionization mode; ^{1}H NMR and ^{13}C NMR spectra – on an AMX-III instrument (Bruker, 400 MHz) in $CDCl_3$ (signals of ^{1}H in $CHCl_3$ was 7.28 ppm, and ^{13}C in $CDCl_3$ was 77.16 ppm); absorption spectra – on a "Cary Spectra 100" spectrophotometer; CD spectra – on a "Jasco-715 CD" spectrometer in $CHCl_3$ using a quartz cell with 1 mm optical path length. Assignment of ambiguous proton resonances in target compounds was performed by analyzing the set of 2D NMR spectra (data not shown).

Testosterone **5** was obtained from "Acros", 3β-(hydroxy)-17-(1H-benzimidazole-1-yl)androsta-5,16-diene (galeterone) from "Selleck". Methyl [17(20)*E*]-6β-methoxy-3α,5α-cyclopregn-17(20)-en-21-oate **7** was synthesized according to procedure [20]; pyropheophorbide a **14** (obtained from methyl pheophorbide) was transformed to pentafluorophenyl pyropheophorbide a **15** according to procedure [21]. Dess-Martin periodinane was synthesized according to procedure [22], other reagents and solvents were purchased from "Aldrich", "Merck", "Acros" and "Fluka".

Flash chromatography was performed on (0.035 – 0.070 mm) silica gel from "Acros", TLC – on HPTLC Silica gel F_{254} GLP 105564 glass plates from 'Merck'; components on the plates were visualized by UV light (Filter 254 nm); and/or by spraying the dried developed plates with 5% $(NH_4)_2MoO_4$ in 10 % sulfuric acid, followed by heating; pyropheophorbide a derivatives were visible on the plates without any treatments.

2.2. CHEMICAL SYNTHESIS

2.2.1. Methyl 6β-methoxy-17α,20(R,S)-epoxy-3α,5α-cyclopregn-17(20)-en-21-oate **8**

m-Chloroperbenzoic acid (2.06 g, 8.37 mmol) was added to the solution of compound **7** (2.00 g, 5.58 mmol) in dichloromethane (60 mL) and the mixture was stirred and heated under reflux for 8 h, the disappearance of starting compound being monitored by TLC. Then saturated solutions of $NaHCO_3$ (70 mL) and $NaHSO_3$ (70 mL) were added; the mixture was vigorously stirred for 30 min; the layers were separated; aqueous layer was extracted with dichloromethane (2 X 30 mL). The combined extract was washed with brine (40 mL), dried over Na_2SO_4, and evaporated. The residue was purified by silica gel flash chromatography in hexane - ethyl acetate (8 : 1) mixture followed by evaporation to obtain epoxide **8** (the mixture of two isomers in a ratio of 3 : 1, 1.34 g, 3.57 mmol, 64%) as colorless glass. HRMS, calculated for $[C_{23}H_{35}O_4]^+$: 375.2530; found: 375.2529. ^{1}H NMR for major isomer: 0.44 and 0.65 (each 1H, m, H-4); 0.93 (3H, s, H-18); 1.00 (3H, s, H-19); 2.78 (1H, t, J = 2.7 Hz, H-6); 3.32 (3H, s, CH_3OC6); 3.45 (1H, s, H-20);

3.75 (3H, s, CH_3OC21); ^1H NMR for minor isomer: 0.44 and 0.65 (each 1H, m, H-4); 0.89 (3H, s, H-18); 1.02 (3H, s, H-19); 2.78 (1H, t, J = 2.7 Hz, H-6); 3.32 (3H, s, CH_3OC6); 3.36 (1H, s, H-20); 3.75 (3H, s, CH_3OC21).

2.2.2. 6β-Methoxy-17α,21-dihydroxy-3α,5α-cyclopregnane **9**

The solution of compound **8** (780 mg, 2.1 mmol) in abs. tetrahydrofuran (20 mL) was added by drops to the stirred suspension of $LiAlH_4$ (175 mg, 4.6 mmol) in abs. tetrahydrofurane (40 mL), then the mixture was stirred and heated under reflux for 2 h. After cooling excess of $LiAlH_4$ was decomposed by adding of ice water. The mixture was filtered, the residue was washed with diethyl ether (2 X 30 mL). The combined extract was dried over Na_2SO_4, and evaporated to obtain diol **9** (680 mg, 1.9 mmol, 90%) as colorless glass. HRMS, calculated for $[C_{22}H_{37}O_3]^+$: 349.2737; found: 349.2732; ^1H NMR: 0.43 and 0.64 (each 1H, m, H-4); 0.74 (3H, s, H-18); 1.03 (3H, s, H-19); 2.76 (1H, m, H-6); 3.32 (3H, s, CH_3O); 3.90 (2H, m, H-21); ^{13}C NMR: 13.2, 16.0, 19.4, 21.6 (C4, C11, C18, C19); 22.4, 23.7, 25.0 (C2, C3, C15); 29.8, 30.8, 30.9, 33.5, 35.3, 36.8(x2), 43.6 (C1, C5, C7, C8, C10, C12, C16, C20); 47.5, 48.1, 49.9 (C9, C13, C14); 56.7 (OCH_3); 61.1 (C21); 82.4 (C6); 85.5 (C17).

2.2.3. 6β-Methoxy-17α-hydroxy-3α,5α-cyclopregnan-21-oic acid **10**

Diol **9** (2.23 g, 6.4 mmol) was dissolved in acetone (120 mL), then $KBrO_3$ (6.4 g, 38.5 mmol), water (80 mL), and RuO_2xH_2O (10 mg) were added, and the mixture was heated under reflux for 20 min, followed by cooling to room temperature. Thereafter ethanol (25 mL) was added by drops, the mixture was filtered, the residue was washed with acetone. The combined filtrate was evaporated, the residue was treated with $CHCl_3$ (150 mL) and water (50 mL). Chloroform extract was washed with brine (50 mL), dried over Na_2SO_4, and evaporated. The residue was applied on the top a silica gel column; the column initially was washed with hexane - ethyl acetate (2 : 1) mixture to remove byproducts, then target compound was eluted with hexane - ethyl acetate - CH_3COOH (50 : 49 : 1) mixture to obtain acid **10** (1.55 g, 4.3 mmol, 67%) as white foam. HRMS, calculated for $[C_{22}H_{35}O_4]^+$: 363.2530; found: 363.2532; ^1H NMR: 0.43 and 0.64 (each 1H, m, H-4); 0.76 (3H, s, H-18); 1.01 (3H, s, H-19); 2.58 (2H, AB system, H-20); 2.78 (1H, m, H-6); 3.32 (3H, s, CH_3O); ^{13}C NMR: 13.2, 16.0, 19.7, 21.6 (C4, C11, C18, C19); 22.2, 23.7, 25.0 (C2, C3, C15); 29.8, 30.8, 33.5, 35.2, 35.3, 37.5 (C1, C5, C7, C8, C12, C16); 39.8, 43.5, 47.5, 47.8, 49.6 (C9, C10, C13, C14, C21); 56.6 (OCH_3); 81.8 (C6); 82.5 (C17); 178.1 (C21).

2.2.4. Ethyl 6β-methoxy-17α-hydroxy-3α,5α-cyclopregnan-21-oate **11**

The mixture of compound **10** (464 mg, 1.28 mmol), N,N'-dicyclohexylcarbodiimide (317 mg, 1.54 mmol), 4-dimethylaminopyridine (220 mg, 1.79 mmol), dry toluene (12 mL), and abs. ethanol (3 mL) was stirred at room temperature for 2.5 h, and then evaporated to dryness. The residue was purified by short column silica gel chromatography in hexane - ethyl acetate (5 : 1) mixture, followed by evaporation to give ester **11** (211 mg, 0.54 mmol, 42%) as colorless glass. HRMS, calculated for $[C_{24}H_{39}O_4]^+$: 391.2843; found: 391.2841; ^{1}H NMR: 0.46 and 0.67 (each 1H, m, H-4); 0.78 (3H, s, H-18); 1.05 (3H, s, H-19); 1.30 (3H, t, J = 7.2 Hz, $\underline{CH_3}CH_2O$) 2.56 (2H, AB system, H-20); 2.79 (1H, t, J = 2.7 Hz, H-6); 3.35 (3H, s, CH_3O); 3.66 (1H, br. s, 17-OH); 4.19 (2H, q, J = 7.1 Hz, $CH_3\underline{CH_2}O$); ^{13}C NMR: 13.1, 14.2, 15.9, 19.3, 21.5 (C4, C11, C18, C19, C23); 22.4, 23.7, 24.9 (C2, C3, C14); 30.7, 30.8, 33.4, 35.2, 35.3 (C1, C7, C8, C12, C16); 37.5, 39.8, 43.4, 47.3, 47.7, 49.5 (C5, C9, C10, C13, C14, C20); 56.6 (OCH_3); 60.6 (C22); 81.6 (C6); 82.4 (C17); 173.8 (C21).

2.2.5. Ethyl 3β,17α-dihydroxypregn-5-en-21-oate **12**

Compound **11** (211 mg, 0.54 mmol) was dissolved in tetrahydrofuran (15 mL), then 15% aqueous H_2SO_4 (4 mL) was added and the mixture was heated under reflux for 20 min. After cooling water (50 mL) was added; the mixture was extracted with $CHCl_3$ (3 X 50 mL); the combined chloroform extract was washed with brine (30 mL), dried over Na_2SO_4, and evaporated to obtain ester **12** (180 mg, 0.48 mmol, 89%) as white powder which was used without purification. The analytical sample was obtained after silica gel flash chromatography in hexane - ethyl acetate (3 : 1) mixture. HRMS, calculated for $[C_{23}H_{37}O_4]^+$: 377.2686; found: 377.2690; ^{1}H NMR: 0.70 (3H, s, H-18); 1.00 (3H, s, H-19); 1.27 (3H, t, J = 7.1 Hz, $\underline{CH_3}CH_2O$); 2.52 (2H, AB system, H-20); 3.50 (1H, m, H-3); 4.16 (2H, q, J = 7.1 Hz, $CH_3\underline{CH_2}O$) 5.34 (1H, m, H-6); ^{13}C NMR: 14.2, 15.5, 19.4, 20.7, 23.9 (C11, C15, C18, C19, C23); 30.3, 31.7, 31.9, 32.3 (C2, C7, C8, C12); 36.6, 37.3, 37.5, 39.8 (C1, C10, C16, C20); 42.3, 46.9, 49.7, 49.9 (C4, C9, C13, C14); 60.7 (C22); 71.7 (C3); 81.6 (C17); 121.6 (C6); 140.7 (C5); 173.7 (C21).

2.2.6. 3-Oxo-17α-hydroxypregn-4-en-21-oic acid **13**

Dess-Martin periodinane (451 mg, 1.06 mmol) was added to the stirred suspension of compound **12** (160 mg, 0.42 mmol) in dichloromethane (20 mL), thereafter water (5 μL, 0.28 mmol) was added and the mixture was stirred for 30 min more, the disappearance of compound **12** during the reaction being controlled by TLC. The mixture was cooled to +4^{o}C, then ethanol (10 mL) was added by drops, the mixture was poured into water (25 mL), extracted with $CHCl_3$ (3 X 10 mL), the extract was washed with brine (30 mL), dried over Na_2SO_4, and evaporated. The residue was dissolved in abs. ethanol (8 mL), then oxalic acid (18 mg, 0.2 mmol) was added, the

mixture was stirred and heating under reflux for 10 min, then poured into water (25 mL). The mixture was extracted with $CHCl_3$ (3 X 10 mL), the extract was washed with brine (30 mL), dried over Na_2SO_4, evaporated, the residue was purified by silica gel flash chromatography in hexane – ethyl acetate (5 : 1) mixture and evaporated to obtain *ethyl 3-oxo-17α-hydroxypregn-4-en-21-oate* (102 mg, 0.27 mmol, 65%) as white solid. ^{1}H NMR: 0.73 (3H, s, H-18); 1.17 (3H, s, H-19); 1.27 (3H, t, J = 7.2 Hz, $\underline{CH_3}CH_2O$); 2.53 (2H, AB system, H-20); 3.62 (1H, br. s, 17-OH); 4.16 (2H, q, J = 7.1 Hz, $CH_3\underline{CH_2}O$); 5.71 (1H, s, H-4). The resulted product was dissolved in methanol (6 mL), then water (4 mL) and K_2CO_3 (400 mg) were added, the mixture was stirred and heated under reflux for 40 min, cooled, then $CHCl_3$ (10 mL) and water (15 mL) were added, the aqueous layer was extracted with $CHCl_3$ (2 X 10 mL); combined chloroform extract was washed with brine (20 mL), dried over Na_2SO_4, evaporated. The residue was purified by silica gel flash chromatography in hexane – acetone - CH_3COOH (64 : 35 : 1) mixture, followed by evaporation to obtain acid **13** (69 mg, 0.2 mmol, 74%) as white solid. HRMS, calculated for $[C_{21}H_{31}O_4]^+$: 347.2217; found: 347.2219; ^{1}H NMR: 0.76 (3H, s, H-18); 1.18 (3H, s, H-19); 2.59 (2H, AB system, H-20); 3.38 (1H, br. s, 17-OH); 5.73 (1H, s, H-4); ^{13}C NMR: 15.5, 17.4, 20.6, 23.7 (C11, C15, C18, C19); 30.2, 32.0, 32.9, 33.9, 35.7, 35.9; 37.4 (C1, C2, C6, C7, C8, C12, C16); 38.7, 39.6, 47.1, 49.0, 53.5 (C9, C10, C13, C14, C20); 81.5 (C17); 123.8 (C4); 171.8 (C5); 177.1 (C21); 200.0 (C3).

2.2.7. Procedure for preparation of amides **16** *and* **17**

The mixture of pentafluorophenyl pyropheophorbide a **15** (210 mg, 0.3 mmol) and diamine (ethylene diamine or 1,5-diaminopentane, 6.0 mmol) and abs. CH_2Cl_2 (10 mL) was stirred for 2 h, then the mixture was poured into 0.1M CH_3COONa buffer, pH 5 (20 mL), extracted with CH_2Cl_2 (2 X 20 mL), the combined extract was washed with brine (20 mL), dried over Na_2SO_4, and evaporated. Then the residue was dissolved in tetrahydrofuran (30 mL), the solution was dried over granulated KOH, followed by evaporation to dryness. Reported [15] *17^3[(2-aminoethyl)amido]pyropheophorbide a* **16** (HRMS, ^{1}H NMR ^{13}C NMR, and absorption spectra data are given in Supplementary data section) was isolated as black amorphous powder (135 mg, 0.22 μmol, 73 %). *17^3[(5-Aminopentyl)amido]-pyropheophorbide a* **17**, purified by flash chromatography in $CHCl_3$: MeOH : NH_4OH (90 : 9 : 1) mixture, was obtained as black amorphous powder (130 mg, 0.21 μmol, 70 %). HRMS, calculated for $[C_{38}H_{47}N_6O_2]^+$: 619.3760; found: 619.3749; ^{1}H NMR: -1.70, 0.40 (each 1H, br.s, N-H); 1.64 (3H, t, J = 7.6 Hz, H-$8^{2'}$); 1.78 (3H, d, J = 7.3 Hz, H-$18^{1'}$); 3.20, 3.38, 3.46 (each 3H, s, H-$2^{1'}$, H-$7^{1'}$, H-$12^{1'}$); 4.30, 4.48 (each 1H, m, H-$17^{1'}$ and H-$8^{1'}$); 5.05 (1H, br. s, NH-CO); 5.05, 5.21 (each 1H, d, J = 19.7 Hz, H-$15^{1'}$); 6.15 (1H, dd, J = 11.5 Hz and J = 1.4 Hz, H-$3^{2'}$, *trans*); 6.26 (1H, dd, J = 17.9 Hz and J = 1.4 Hz,

H-3$^{2'}$, *cis*); 7.96 (1H, dd, J = 11.5 Hz and J = 17.9 Hz, H-3$^{1'}$); 8.53, 9.31, 9.34 (each 1H, s, H-5', H-10', H-20'); ^{13}C-NMR: 11.3, 11.9, 12.2, 17.5, 19.5 (C2$^{1'}$, C7$^{1'}$, C8$^{1'}$, C8$^{2'}$, C12$^{1'}$); 23.2, 24.0, 29.1 (C5'', C6'', C18$^{1'}$); 30.3, 32.9, 33.0, 39.3, 41.8 (C3'', C4'', C7'', C17$^{1'}$, C17$^{2'}$); 48.1, 50.1, 51.8 (C15$^{1'}$, C17', C18'); 93.0, 97.2, 104.1, 106.2 (C5', C10', C15', C20'); 122.6 (C3$^{2'}$); 128.3, 129.3, 130.5 (C3$^{1'}$, C11', C13'); 131.6, 135.9, 136.1, 136.2, 137.8 (C2', C3', C4', C7', C12'); 141.6, 145.1, 149.0 (C8', C14', C16'); 150.8, 155.3, 160.5, 171.9, 172.1 (C1', C6', C9', C17$^{3'}$, C19'); 196.2 (C13$^{1'}$), absorption spectrum – in Figure 2.

2.2.8. Procedure for preparation of conjugates **1 – 4**

The mixture of carboxylic acids (**6** or **13,** 0.1 mmol), amine **(16** or **17,** 0.1 mmol), and N,N'-dicyclohexylcarbodiimide (23 mg, 0.11 mmol) in dichloromethane (5 mL) was stirred at room temperature for 2 h, then evaporated to dryness, and the residue was applied on the top a silica gel column. The column initially was washed with $CHCl_3$ – acetone - CH_3COOH (75 : 24 : 1) mixture to remove byproducts, then washed with 5 mL $CHCl_3$, and finally the target product was eluted with $CHCl_3$ – methanol - 7M solution of NH_3 in methanol (93 : 5 : 2, by vol.) mixture. After evaporation the conjugates were dried in vacuo.

2.2.9. 17^3[2-(17β-Hydroxy-3-oxopregn-4-en-21-oylamidoethyl)amido]pyropheophorbide a **1**

Reported [15] conjugate **1** (38 mg, 42 μmol, 42 %) was obtained as black powder. HRMS, calculated for $[C_{56}H_{69}N_6O_5]^+$: 905.5329, found: 905.5327, ^{1}H NMR and ^{13}C NMR data are presented in Supplementary data, absorption spectrum – in Figure 2.

2.2.10. 17^3[5-(17β-Hydroxy-3-oxopregn-4-en-21-oylamidopentyl)amido]pyropheophorbide a **2**

Conjugate **2** (48 mg, 51 μmol, 51%) was obtained as black powder. HRMS, calculated for $[C_{59}H_{75}N_6O_5]^+$: 947.5793; found: 947.5789; ^{1}H NMR: -1.66 (1H, br. s, N-H); 0.73, 1.00 (each 3H, s, H-18 and H-19); 1.64 (3H, t, J = 7.6 Hz, H-8$^{2'}$); 1.78 (3H, d, J = 7.3 Hz, H-18$^{1'}$); 3.19, 3.37, 3.46 (each 3H, s, H-2$^{1'}$, H-7$^{1'}$, H-12$^{1'}$); 4.27, 4.46 (each 1H, m, H-17$^{1'}$ and H-8$^{1'}$); 5.00, 5.16 (each 1H, d, J = 19.7 Hz, H-15$^{1'}$); 5.28 (1H, br. t, J = 5.2 Hz, NH-CO); 5.53 (1H, s, H-4); 6.15 (1H, dd, J = 11.5 Hz and J = 1.4 Hz, H-3$^{2'}$, *trans*); 6.25 (1H, dd, J = 17.9 Hz and J = 1.4 Hz, H-3$^{2'}$, *cis*); 6.33 (1H, br. t, J = 5.2 Hz, NH-CO); 7.94 (1H, dd, J = 11.5 Hz and J = 17.9 Hz, H-3$^{1'}$); 8.51, 9.28, 9.31 (each 1H, s, H-5', H-10', H-20'); ^{13}C NMR: 11.3, 12.0, 12.2, 13.9 (C2$^{1'}$, C7$^{1'}$, C12$^{1'}$, C18); 17.3, 17.5, 19.5 (C8$^{1'}$, C8$^{2'}$, C19); 20.6, 23.1, 23.6, 23.9, 28.8, 29.0 (C4'', C5'', C6'', C11, C15, C18$^{1'}$); 29.8, 30.5, 31.7, 32.7, 33.1, 33.9 (C2, C6, C7, C12. C17$^{1'}$, C17$^{2'}$); 35.7, 36.2, 36.5, 38.6, 39.0, 39.1 (C1, C3'', C7'', C8, C10, C16); 42.6, 46.2, 48.1 (C13, C15$^{1'}$, C20); 50.1 (x2), 51.7, 53.8 (C9, C14, C17', C18'); 82.0 (C17); 93.1, 97.3, 104.1, 106.0 (C5',

C10', C15', C20'); 122.7, 123.8, 128.2, 129.2 (C3$^{1'}$, C3$^{2'}$, C4, C11'); 130.3, 131.8, 136.0, 136.2, 136.4, 137.8 (C2', C3', C4', C7', C12', C13'); 141.8, 145.2, 149.1, 150.9, 155.5 (C6', C8', C9', C14', C16'); 160.5, 171.0, 172.0, 172.5, 173.4 (C1', C5, C17$^{3'}$, C19', C21); 196.3 (C13$^{1'}$), 199.4 (C3); absorption spectrum is presented in Figure 2.

***2.2.11. 17^3[2-(17α-Hydroxy-3-oxopregn-4-en-21-oylamidoethyl)amido]pyropheophorbide a* 3**

Conjugate **3** (28 mg, 31 μmol, 31%) was obtained as black powder. HRMS, calculated for $[C_{56}H_{69}N_6O_5]^+$: 905.5329, found: 905.5335; ^{1}H NMR: -1.67 (1H, br. s, N-H); 0.54, 0.88 (each 3H, s, H-18 and H-19); 1.55 (3H, t, J = 7.7 Hz, H-8$^{2'}$); 1.75 (3H, d, J = 7.3 Hz, H-18$^{1'}$); 3.13, 3.15, 3.35 (each 3H, s, H-2$^{1'}$, H-7$^{1'}$, H-12$^{1'}$); 4.20, 4.45 (each 1H, m, H-17$^{1'}$ and H-8$^{1'}$); 4.92, 5.15 (each 1H, d, J = 19.7 Hz, H-15$^{1'}$); 5.53 (1H, s, H-4); 6.11 (1H, dd, J = 11.6 Hz and J = 1.4 Hz, H-3$^{2'}$, *trans*); 6.25 (1H, dd, J = 17.8 Hz and J = 1.4 Hz, H-3$^{2'}$, *cis*); 6.24 (1H, br. t, J = 5.2 Hz, NH-CO); 6.78 (1H, br. t, J = 5.2 Hz, NH-CO); 7.88 (1H, dd, J = 11.6 Hz and J = 17.8 Hz, H-3$^{1'}$); 8.58, 9.10, 9.24 (each 1H, s, H-5', H-10', H-20'); ^{13}C NMR: 11.2, 11.6, 12.1 (C2$^{1'}$, C7$^{1'}$, C12$^{1'}$); 15.1, 16.9, 17.3 (C8$^{2'}$, C18, C19); 19.3, 20.1, 23.0, 23.3, 29.9, 30.5 (C8$^{1'}$, C11, C12, C15, C17$^{1'}$, C18$^{1'}$); 31.6, 32.6, 33.0, 33.7, 35.2, 35.5 (C1, C2, C6, C7, C8, C17$^{2'}$); 37.0, 38.2, 39.6, 40.0, 40.5 (C3'', C4'', C10, C16, C20); 46.5, 48.1, 48.5, 50.1, 51.7, 53.0 (C9, C13, C14, C15$^{1'}$, C17', C18'); 81.6 (C17); 93.0, 97.1, 103.9, 105.8 (C5', C10', C15', C20'); 122.7, 123.6, 127.8, 129.0 (C3$^{1'}$, C3$^{2'}$, C4, C11'); 129.9, 131.7, 135.9, 136.0, 136.3, 137.6 (C2', C3', C4', C7', C12', C13'); 141.7, 145.1, 148.9, 150.8, 155.4 (C6', C8', C9', C14', C16'); 160.2, 171.2, 171.9, 173.6, 173.8 (C1', C5, C17$^{3'}$, C19', C21); 196.3 (C13$^{1'}$); 199.3 (C3); absorption spectrum is presented in Figure 2.

***2.2.12. 17^3[5-(17α-Hydroxy-3-oxopregn-4-en-21-oylamidopentyl)amido]pyropheophorbide a* 4**

Conjugate **4** (44 mg, 46 μmol, 46%) was obtained as black powder. HRMS, calculated for $[C_{59}H_{75}N_6O_5]^+$: 947.5793; found: 947.5793; ^{1}H NMR: -1.67 (1H, br. s, N-H); 0.25, 0.81 (each 3H, s, H-18 and H-19); 1.61 (3H, t, J = 7.6 Hz, H-8$^{2'}$), 1.78 (3H, d, J = 7.3 Hz, H-18$^{1'}$), 3.17, 3.36, 3.37 (each 3H, s, H-2$^{1'}$, H-7$^{1'}$, H-12$^{1'}$); 4.26, 4.46 (each 1H, m, H-17^1 and H-8$^{1'}$); 5.00, 5.15 (each 1H, d, J = 19.7 Hz, H-15$^{1'}$); 5.53 (1H, br. t, J = 5.2 Hz, NH-CO); 5.58 (1H, s, H-4); 6.14 (1H, dd, J = 11.5 Hz and J = 1.4 Hz, H-3$^{2'}$, *trans*); 6.22 (1H, br. t, J = 5.2 Hz, NH-CO); 6.23 (1H, dd, J = 17.9 Hz and J = 1.4 Hz, H-3$^{2'}$, *cis*); 7.92 (1H, dd, J = 11.5 Hz and J = 17.9 Hz, H-3$^{1'}$); 8.50, 9.24, 9.32 (each 1H, s, H-5', H-10', H-20'); ^{13}C NMR: 11.3, 11.9, 12.1 (C2$^{1'}$, C7$^{1'}$, C12$^{1'}$); 15.2, 17.1, 17.4, 19.4 (C8$^{1'}$, C8$^{2'}$, C18, C19); 20.3, 23.1, 23.4, 23.7, 28.5, 28.9 (C4'', C5'', C6'', C11, C15, C18$^{1'}$); 30.2, 30.6, 31.8, 32.0, 33.1, 33.9 (C2, C6, C7, C12, C17$^{1'}$, C17$^{2'}$); 35.4, 35.7, 37.1, 38.4, 38.9, 39.0, 40.3 (C1, C3'', C7'', C8, C10, C16, C20); 46.6, 48.1, 48.7, 50.1, 51.7,

53.2 (C9, C13, C14, $C15^{1'}$, C17', C18'); 81.8 (C17), 93.1, 97.2, 104.0, 105.9 (C5', C10', C15', C20'); 122.7, 123.7, 128.1, 129.1 ($C3^{1'}$, $C3^{2'}$, C4, C11'); 130.2, 131.8, 136.0, 136.2, 136.4, 137.8 (C2', C3', C4', C7', C12', C13'); 141.7, 145.2, 149.0, 150.8, 155.4 (C6', C8', C9', C14', C16'); 160.5, 171.5, 172.0, 172.8, 173.1 (C1', C5, $C17^{3'}$, C19', C21); 196.3 ($C13^{1'}$); 199.6 (C3); absorption spectra in $CHCl_3$ is presented in Figure 2.

2.3. MOLECULAR MODELING

Conformation searches have been performed using molecular mechanics MMFF94 force field parameters in vacuo. OpenBabel package [23] was employed for initial structure preparation and energy minimizations. Simulated annealing molecular dynamics (MD) has been performed to sample low-energy conformation space of compounds **1 – 4**, using NAMD [24] software. Parameters and topology files were generated with the aid of SwissParam server [25] on the basis of MMFF94 force field. The annealing protocol consisted of 4 ps high temperature runs at 500 K followed by 4 ps cooling phase bringing temperature down to 50 K, with total of 200 annealing cycles scheduled in 32 processes. This procedure yielded 6400 local energy minima for each compound. Resulting structures were then optimized by energy minimization with MMFF94 potential. VMD package [26] was used for MD trajectory post-processing, analysis, and visualization.

2.4. BIOLOGICAL EVALUATION

2.4.1. Cell Cultures

The human prostate cancer cells LNCaP and PC-3 were obtained from the American Type Culture Collection (Rockville, MD). Cells were propagated in culture dishes at the desired densities in RPMI 1640 medium supplemented with 10% fetal calf serum (FCS; Gibco, Grand Island, NY) and 1% penicillin/streptomycin (Gibco) in a 5% CO_2 atmosphere at 37^{o}C for 24 h. (Concentrations of cations in the medium were as follows: Ca^{2+} - 5.74 X 10^{-4} M, Mg^{2+} - 4.06 X 10^{-4} M, K^+ - 5.36 X 10^{-3} M, Na^+ - 0.132 M; the medium did not contained ions: Zn^{2+}; Mn^{2+}; Mn^{3+}; Mn^{4+}). Before experiments the cells were seeded either in 96-well plates at a density of $5 \cdot 10^3$ cells/well (for MTT assay), or in 6-well plates at a density of 10^6 cells/well (for investigation of uptake and internalization of conjugates) and incubated for 48 h.

2.4.2. Uptake and internalization of conjugates* 1 - 4 *by prostate carcinoma cells.

LNCaP cells in a 6-well plates were incubated for 2, 6, 14 and 20 h with conjugates **1 – 4** (25 μM in culture medium), then medium was aspirated, cells were washed with cold PBS at 4^o C, and lipids from each well were extracted with hexane – isopropanol mixture (3 : 2, 3 x 0.5 mL).

Pellets were used for cell protein concentration measurements [27]. Lipid extracts were dried under nitrogen flow, residues were dissolved in CH_2Cl_2 (2 mL), and concentrations of conjugates were determined spectrophotometrically. All measurements were carried out in triplicates. The efficiency of cell labeling was expressed in terms of ratios of internalized conjugates (nmol per mg of cell protein).

Galeterone effect on uptake of conjugates was determined by using LNCaP and PC-3 cells preincubated with galeterone (10 μM) for 14 h, followed by incubation with conjugates (25 μM) for 6 h in the presence of galeterone (10 μM), and quantification of conjugates in cell extract as indicated above.

2.4.3. MTT cell viability assay [28]

LNCaP and PC-3 cells were treated with conjugates **1 – 4** at the designated concentrations, and incubated for 96 h in 96-well plates. Then, solution of 3-(4,5-dimethylthiazol-2-yl)-2,5-diphenyltetrazolium bromide (MTT) (5 mg/mL) was added and the cells were incubated for 4 h, followed by measuring absorbance at 570 nm, with "Techan Genius plus" microplate reader. The viability of treated cells was expressed as a percentage relative to that of control cells. Each experiment was performed in triplicate, and independently repeated at least four times.

RESULTS AND DISCUSSION

3.1. Chemical synthesis.

Synthesis of compounds **1 – 4** was performed according to Scheme 1 consisting of preparation of 17β-hydroxy- and 17α-hydroxy- acids **6** and **13**, and coupling aforementioned acids with pyropheophorbide a **14** by means of either ethylene diamine, or 1,5-diamino pentane linkers.

17β-Hydroxy-3-oxopregn-4-en-21-oic acid **6** was prepared in 49 % overall yield from testosterone **5** in five steps, including consecutive protection of carbonyl function with formation of 1,3-dioxolane, oxidation of 17β-hydroxyl group, Reformatsky reaction of obtained 17-ketone with Zn and ethyl bromoacetate, and removal of protective groups [29-31] (Supplementary data).

Synthesis of 17α-hydroxy-3-oxopregn-4-en-21-oic acid **13** was carried out from reported earlier methyl ester **7** [16]; the key step – introducing of 17α-hydroxyl group – was performed according to known approach based on peracid oxidation of 17(20)-pregnenes to 17α,20-epoxides followed by their reduction to 17α-hydroxyl containing pregnanes [29, 32].

Treatment of compound **7** with excess of m-chloroperbenzoic acid in boiling dichloromethane during 8 h resulted in epoxide **8** in 64 % yield. Epoxide **8** was isolated as mixture of related 17α,20(*R*)- and 17α,20(*S*)- isomers in ratio of 3 : 1 (according to ^{1}H NMR spectra, section **2.2.1**). Reduction of the crude epoxide **8** with $LiAlH_4$ in boiling tetrahydrofurane during 2 h gave 17α,21-diol **9** in near quantitative yield. Diol **9** was transformed to hydroxy acid **10** by oxidation with ruthenate - potassium bromate reagent [33] in acetone solution (68% yield). Esterification of carboxylic group of compound **10** led to ethyl ester **11**, which was subjected to acid hydrolysis to obtain 3β-hydroxy-5-en ester **12** in overall 37 % yield (based on **10**). Oxidation of compound **12** with Dess-Martin periodinane, followed by acid catalyzed isomerization of crude 3-oxo-5-ene derivative and subsequent alkali hydrolysis of ester group, resulted in target 17α-hydroxy-3-oxopregn-4-en-21-oic acid **13** in 48 % overall yield (based on **12**).

Both 17β-hydroxy- and 17α-hydroxy acids **6** and **13** were obtained as pure compounds, and configuration of C17 was confirmed by ^{13}C NMR spectra. The differences in chemical shifts of C16, C17, and C18 resonances in compounds **6** and **13** were considered to be in agreement with published data of ^{13}C NMR spectra for related 17α- and 17β-hydroxyestradiols [34].

Pyropheophorbide a derivatives comprising primary amino group (compounds **16** and **17**) were prepared from pyropheophorbide a **14** through formation of pentafluorophenyl ester **15** [21], followed by its treatment with excess of either ethylene diamine, or 1,5-diaminopentane. Condensation of steroid acids **6** and **13** with amines **16** and **17** in the presence of N,N-dicyclohexylcarbodiimide led to the target conjugates **1 – 4**.

3.2. Spectral properties and molecular models

Absorption spectra of conjugates **1 – 4** (Figure 2) were similar to each other and were typical for pyropheophorbide a **14** and their derivatives; CD spectra of conjugates **1 – 4** (Figure 3) also did not display any significant differences caused by structural peculiarities.

We have observed strong high-field shifts of some resonances in ^{1}H-NMR spectra of conjugates **1 – 4** in comparison with those in spectra of non-conjugated steroidal acids **6** and **13** (Table 1). The observed high field shifts for H-4, H-18, H-19 in conjugates were clearly caused by influence of macrocycle on steroid moiety. The greatest high field shift for H-4 resonance was observed in spectra of conjugates **2** and **3**, while that for H-18 resonance – in spectra of conjugates **1** and **4**. In addition, we have observed that amide N-H resonances in spectra of conjugates **1** and **3** were shifted into low field in comparison to conjugates **2** and **4**. Due to the longer linker lengths in conjugates **2** and **4**, they exhibit much greater conformational flexibility (Figure 4), which allows more conformers with N-H proton axially positioned off the macrocycle plane, pushing corresponding NMR resonances into higher field. Because position of steroid moiety in the lowest-energy conformers was found to be not significantly different between conjugates with different linker lengths, we concluded that the main effect of linker lengthening is, indeed, enhanced conformational flexibility. Configuration of C17 affects the relative positioning of 17-hydroxy group, and in epitestosterone conjugates **3** and **4** this group was found to be oriented towards the macrocycle (Figure 4), and is capable of hydrogen bond formation with nearby amide proton (Figure 5). On the contrary, in testosterone derivatives **1** and **2** mentioned hydroxy group is directed outwards from the macrocycle, and completely exposed to the environment. Chemical shifts for H-5', H-10' and H-20' resonances in pyropheophorbide moieties of conjugates **1**, **2**, **3** and **4** also differed significantly. The data presented in the Table 1 are thought to be in agreement with results of molecular modeling indicated differences in positional relationships of steroid and macrocycle moieties in conjugates **1 - 4**.

Molecular modeling of compounds **1 - 4** was performed by simulated annealing. Calculated ensembles of conformers, truncated at 10 kcal/mol above lowest-energy conformer, are shown on the Figure 4; lowest energy conformers are presented on Figure 5.

Structures with steroid moiety hoisted over the surface of macrocycle were found energetically favorable in all cases. This 'folded' structure correlates well with observed high-field shifts of 18- and 19-methyl protons compared to unconjugated steroids, because of shielding effect exerted by large aromatic moiety of pyropheophorbide on atoms located above and below its surface. Presence of 'unfolded' conformers with relatively low energy in

compounds 2 and 3 (Figure 4) is probably responsible for the observed weaker shielding of 18- and 19-methyls (Table 1), due to less stability of 'folded' conformation.

Conformers presented in the Figure 5 are partially stabilized by possibility of intramolecular hydrogen bonds formation. In the lowest energy conformers of conjugates **1** and **2** nitrogen atom N(1") is located near carbonyl group of pyrophreophorbide a, thus making formation of corresponding hydrogen bond favorable. Additionally, in compound **1** the oxygen atom of 21-amide group is located between 17β-hydroxyl group and nitrogen atom N(2") of ethylene diamine linker, and thus can serve as proton acceptor with either of these atoms being a donor. In the lowest energy conformers of conjugates **3** and **4** 17α-hydroxyl group is located close to nitrogen atom N(1"), and apparently may serve as proton acceptor to form the corresponding hydrogen bond. Generally, modeling results reveals a disposition of conjugates **1 – 4** to support intramolecular hydrogen bond network, which contributes to the apparent stability of 'folded' conformers, especially in hydrophobic environments where no external proton donors are present.

3.3. Biological evaluation

Conjugates **1 – 4** were evaluated for their uptake and internalization in prostate carcinoma LNCaP cells. These cells express only one steroid receptor (mutant androgen receptor T877A [35,36]), and presents an appropriate model for studies of androgen-sensitive cells. Time course of conjugates uptake by LNCaP cells is given in Figure 6. Epitestosterone derivatives were uptaken more efficiently than testosterone ones; in both pairs conjugates comprising shorter linkers were uptaken more efficiently than those comprising long linkers (**3 > 4 ≥ 1 > 2**). According to our molecular models (Section **3.2**), this dependence must be correlated to diminished conformational flexibility of compounds **1** and **4**, combined with predominant 17-hydroxy group exposure in testosterone derivatives. The internalization of conjugates by cells was confirmed as follows: LNCaP cells, initially labeled with conjugates **1 – 4** for 6 h, were incubated for 12 h in fresh medium, followed by determination of conjugates content in it. The absence of detectable amounts of conjugates in the medium proves that they were completely internalized by cells.

Speculating that steroid fragment of conjugates may affect their binding to cells, we compared interaction of conjugate **3** with LNCaP cells either in the presence, or in the absence of galeterone, the known androgen receptor antagonist and degrading agent [37]. Initially, we presumed that galeterone could compete with conjugate for binding to LNCaP cells and could decrease uptake and internalization of conjugate, since activity of androgen receptor was blocked.

However, experimental data demonstrated that galeterone treatment significantly stimulated uptake and internalization of conjugate **3** in LNCaP cells (Figure 7A). The enhanced uptake of conjugate **3** by LNCaP cells most probably can't be caused by effects of galeterone on androgen receptor pathway, but by participation of galeterone in other regulatory processes. To check this hypothesis we investigated an effect of galeterone treatment on uptake and internalization of conjugates **1**, **2**, **4**, and synthesized earlier [19] steroid-free conjugate 17^3[(2'-tert-butyloxycarbonylamidoethyl)amido]-pyropheophorbide a **18** in androgen insensitive PC-3 cells (Figure 7B). Galeterone treatment enhanced uptake of all conjugates in PC-3 cells.

Figures 7A and 7B clearly showed that galeterone treatment enhanced uptake of all conjugates independently on their structure and activity of androgen receptor.

We have found that conjugates **1 – 4 (**in concentrations up to 50 μM) slightly inhibited the growth of LNCaP and PC-3 cells at 24 h incubation, however potently inhibited it at prolong incubation. MTT test data demonstrating effects of conjugates **1 – 4** on the viability of LNCaP and PC-3 cells at 96 h incubation are presented in Supplementary data section; the related IC_{50} values are given in the Table 2. Conjugates inhibited growth of both LNCaP and PC-3 cells, however, effect on LNCaP cells was more pronounced. Anti-proliferative activity of conjugates in LNCaP and PC-3 cells was dependent on the structure of steroid moiety and length of linker and decreased in the row: **3 > 1 > 4 > 2.** The most potent inhibitor was epitestosterone derivative comprising short linker **3**, the less potent – testosterone derivative comprising long linker **2**.

Obtained results revealed that structural peculiarities of conjugates **1 – 4** affect their binding to prostate carcinoma cells and manifestation of their anti-proliferative ability. Nevertheless, these conjugates can't be considered as agents for targeting androgen receptor. Our docking studies also revealed that conjugates **1 – 4** can't form a complexes with ligand binding domain of androgen receptor due to steric hindrances of bulk pyropheophorbide a fragments (data not presented). In addition, conjugates **1 – 4** may be used as probes for fluorescent imaging of prostate carcinoma cells; these studies are in progress in our team, and the results will be presented elsewhere.

Conclusions.

Four conjugates of 17-substituted testosterone and epitestosterone with pyropheophorbide a comprising either ethylene diamine, or 1,5-diaminopentane linkers were synthesized. Spectral characteristics and molecular models of conjugates revealed that mutual influence of steroidal and macrocyclic moieties were dependent on configuration of C17 and length of linker. The uptake, internalization, and anti-proliferative activity of conjugates in prostate carcinoma LNCaP and PC-3 cells were found to be dependent on their structure as well. Epitestosterone derivative

comprising short linker exhibited the maximal activity. Molecular models reveal that the main effect of the longer linker is enhanced conformational flexibility of compounds **1** and **3**, therefore conjugates **2** and **3**, showing stronger biological effects, were conformationally more rigid ones. On the other hand, configuration of C17 mainly affects relative position of 17-hydroxy group relative to the macrocycle, and the more potent compounds have this group predominantly shielded from the environment, as it is flanked by pyropheophorbide a macrocycle on one side, steroid moiety on the other, and involved in hydrogen bonding with linker amide group located nearby. Therefore, those compounds with this group completely exposed to solution (**1** and **2**) were found to be less active against prostate carcinoma LNCaP and PC-3 cells relatively to their corresponding counterparts. Galeterone treatment enhanced uptake of all conjugates independently on their structure, so uptake of conjugates is considered to be androgen receptor independent.

Acknowledgments.

Authors are acknowledged to Dr. Vladimir F. Pozdnev, Dr. Alexander V. Veselovsky, Dr. Alexey V. Kuzikov, Alexandra S. Latysheva and Rami A. Masamrekh (all from Orekhovich Institute of Biomedical Chemistry) for essential assistance and fruitful discussion, and to Dmitry N. Kaluzhny (Engelhardt Institute of Molecular Biology*)* for recording of CD spectra. This study was supported by State Academies of Sciences Fundamental Research Program for 2013–2020 years (for chemical synthesis and biological studies - № 051820140003; for molecular modeling and spectroscopic studies - № 01201363818), and partially by Russian Foundation for Basic Research (grants №15-04-02939_a; №15-04-02426_a; №16-04-00293_a).

REFERENCES

1. J.A. Katzenellenbogen, B.S. Katzenellenbogen, Considerations in the design and evaluation of cytotoxic estrogens, Breast Cancer Res. Treat. 2 (1982) 347–53.
2. H.Y. Lam, G.J. Goldenberg, C.M. Wong, Interaction of estrogen-nitrosourea conjugates with the estrogen receptor in rat uterus, Biochem. Pharmacol. 37 (1988) 2625–31.
3. M. Georgiadis, K.P. Chondros, S.A. Haroutounian, Synthesis and biological studies of steroidal cis-platinum (II) complexes, Inorg. Chim. Acta 138 (1987) 249–52.
4. J. Quivy, G. Leclerq, M. Deblaton, P. Henrot, N. Velings, B. Norberg, G. Evrard, M. Zeicher, Synthesis, structure and biological properties of Z-17α-(2-iodovinyl)-11β-chloromethyl estradiol-17β (Z-CIMIV), a high affinity ligand for the characterization of estrogen receptor positive tumors, J. Steroid Biochem. Mol. Biol. 59 (1996) 103–17.
5. H. Akaza, S. Imada, S. Tsukamoto, K. Koiso, Inhibitory effects of bestrabucil, a conjugate of chlorambucil and estradiol, on the production of androgen-induced growth factors by Shiongi carcinoma 115 cells, Int. J. Urol. 1 (1994) 67–73.
6. R. Devraj, J. Barett, J.A. Fernandez, J.A. Katzenellenbogen, M. Cushman, Design, synthesis and biological evaluation of ellipticine-estradiol conjugates, J. Med. Chem. 39 (1996) 3367–74.
7. D. Bastien, R. Hanna, V. Leblanc, E. Asselin, G. Bérubé, Synthesis and preliminary in vitro biological evaluation of 7α-testosterone-chlorambucil hybrid designed for the treatment of prostate cancer, Eur. J. Med. Chem. 64 (2013) 442-7.
8. P. Saha, C. Debnath, G. Bérubé, Steroid-linked nitrogen mustards as potential anticancer therapeutics: A review, J. Steroid Biochem. Mol. Biol. 137 (2013) 271–300.
9. G. Bérubé, An overview of molecular hybrids in drug discovery, Expert Opin. Drug Disc. (2016) DOI: 10.1517/17460441.2016.1135125.
10. P.M. Levine, M.J. Garabedian, K. Kirshenbaum, Targeting the androgen receptor with steroid conjugates, J. Med. Chem. 57 (2014) 8224-37
11. W. Zhu, L.X. Wang, D.Y. Chen, Y.H. Gao, Y.J. Yan, X.F. Wu, M. Wang, Y.P. Han, Z.L. Chen, Synthesis and biological evaluation of 17^3-dicarboxylethyl-pyropheophorbide a amide derivatives for photodynamic therapy, Bioorg. Med. Chem. Lett. (2017) doi:10.1016/j.bmcl. 2017.12.034.
12. X. Zhang, Q. Yan, D.N. Mulatihan, J. Zhu, A. Fan, Z. Wang, Y. Zhao, Pharmaceutical micelles featured with singlet oxygen-responsive cargo release and mitochondrial targeting for enhanced photodynamic therapy. Nanotechnology 29 (2018) 255101.

13. W. Li, S. Tan, Y. Xing, Q. Liu, S. Li, Q. Chen, M. Yu, F. Wang, Z. Hong, cRGD-Peptide-conjugated pyropheophorbide a photosensitizers for tumor targeting in photodynamic therapy, Mol. Pharm. 15 (2018) 1505-14.
14. L. Liang, W. Bi, W. Chen, Y. Lin, Y. Tian, Combination of MPPa-PDT and HSV1-TK/GCV gene therapy on prostate cancer, Laser Med. Sci. 33 (2018) 227-32.
15. E.H. Khan, H. Ali, H. Tian, J. Rousseau, G. Tessier, Shafiullah, J.E. van Lier, Synthesis and biological activities of phthalocyanine–estradiol conjugates, Bioorg. Med. Chem. Lett. 13 (2003) 1287-90.
16. H.A. Zhylitskaya, V.N. Zhabinskii, R.P. Litvinovskaya, R. Lettieri, D. Monti, M. Venanzi, V.A. Khripach, P. Drašar, Design and studies of novel polyoxysterol-based porphyrin conjugates, Steroids 77 (2012) 1169-75.
17. J. Koivukorpi, E. Sievänen, E. Kolehmainen, V. Král, Synthesis, characterization, and saccharide binding studies of bile acid − porphyrin conjugates, Molecules 12 (2007) 13-24.
18. S. Sadler, K.S. Persons, G.B. Jones, R. Ray, Internalization of a C17α-alkynylestradiol-porphyrin conjugate into estrogen receptor positive MCF-7 breast cancer cells, Bioorg. Med. Chem. Lett. 21 (2011) 4638-41.
19. V.A. Zolottsev, O.V. Zazulina, G.E. Morozevich, M.G. Zavialova, A.Y. Misharin, R.A. Novikov, V.P. Timofeev, O.I. Koifman, G.V. Ponomarev, Conjugates of pyropheophorbide a with androgen receptor ligands, Macroheterocycles 10 (2017) 77-80.
20. V.A. Zolottsev, Y.V. Tkachev, A.S. Latysheva, V.A. Kostin, R.A. Novikov, V.P. Timofeev, G.E. Morozevich, A.V. Kuzikov, V.V. Shumyantseva, A.Y. Misharin, Comparison of [17(20)*E*]-21-Norpregnene oxazolinyl and benzoxazolyl derivatives as inhibitors of CYP17A1 activity and prostate carcinoma cells growth, Steroids 129 (2018) 24-34.
21. I.A. Nikolaeva, J.V. Morozova, M.G. Zavialova, R.A. Novikov, Y.V. Tkachev, V.P. Timofeev, A.Y. Misharin, G.V. Ponomarev, Natural chlorins modified with cholesterol moiety. Synthesis, characteristics, copper complexes, and entrapping in phospholipid vesicles, Macroheterocycles 3 (2010) 150-6.
22. G. Tojo, M. Fernandez, Oxidation of Alcohols to Aldehydes and Ketones, Springer, NY (2006) Chapter 3 pp 181-200.
23. The Open Babel Package, version 2.0.1, http://openbabel.sourceforge.net/
24. J.C. Phillips, R. Braun, W. Wang, J. Gumbart, E. Tajkhorshid, E. Villa, C. Chipot, R.D. Skeel, L. Kale, K. Schulten, Scalable molecular dynamics with NAMD, J. Comput. Chem. 26 (2005) 1781-1802.
25. V. Zoete, M.A. Cuendet, A. Grosdidier, O. Michielin, SwissParam, a Fast Force Field Generation Tool For Small Organic Molecules, J. Comput. Chem. 32 (2011) 2359-68.

26. W. Humphrey, A. Dalke, K.J. Schulten, VMD: Visual molecular dynamics, Molec. Graphics, 14 (1996) 33.
27. P.K. Smith, R.I. Krohn, G.T. Hermanson, A.K. Mallia, F.H. Gartner, M.D. Provenzano, E.K. Fujimoto, N.M. Goeke, B.J. Olson, D.C. Klenk, Measurement of protein using bicinchoninic acid, Anal. Biochem. 150 (1985) 76-85.
28. T. Mosmann, Rapid colorimetric assay for cellular growth and survival: application to proliferation and cytotoxicity assays, J. Immunol. Methods 65 (1983) 55–63.
29. E.P. Oliveto in: Organic reactions in steroid chemistry. J. Fried, J.A. Edwards, eds. Van Nostrand Reinhold Co (1972) vol.2, 127-236, and the references therein.
30. A. Liu, K.E. Carlson, J.A. Katzenellenbogen, Synthesis of high affinity fluorine-substituted ligands for the androgen receptor potential agents for imaging prostatic cancer by positron emission tomography, J. Med. Chem. 35 (1992) 2113-29.
31. D. Bittler, H. Laurent, P. Rach, M. Topert, Androstane derivatives, US Patent 5010071, Apr 23 (1991)
32. M. Lewbart, Preparation and properties of β-lactones from steroidal 17,20-dihydroxy-21-oic acids, J. Org. Chem. 37 (1972) 1224-32.
33. A.E.M. Boelrijk, J.J. Reedijk, Oxidation of methyl- and octyl-α-D-glucopyranoside, catalyzed by high-valent ruthenium species, J. Mol. Catal. 89 (1994) 63-76.
34. P. Dionne, B.T. Ngatcha, D. Poirier, D-ring allyl derivatives of 17β- and 17α-estradiols: Chemical synthesis and ^{13}C NMR data, Steroids 62 (1997) 674-81.
35. J.S. Horoszewicz, S.S. Leong, E. Kawinski, J.P. Karr, H. Rosenthal, Chu T. Ming, E.A. Mirand, G.P. Murphy, LNCaP model of human prostatic carcinoma, Cancer Res. 43 (1983) 1809-18.
36. E.M. Berns, W. De Boer, E. Mulder, Androgen-dependent growth regulation of and release of specific protein(s) by the androgen receptor containing human prostate tumor cell line LNCaP, Prostate 9 (1986) 247-59.
37. V.C. Njar, A.M. Brodie, Discovery and development of Galeterone (TOK-001 or VN/124-1) for the treatment of all stages of prostate cancer, J. Med. Chem. 58 (2015) 2077-87.

LEGENDS TO FIGURES

Figure 1. Conjugates **1 – 4**.

Figure 2. Normalized absorption spectra of conjugates **1** (olive); **2** (purple); **3** (blue); **4** (red) in $CHCl_3$.

Figure 3. CD spectra of conjugates **1**(olive); **2** (purple); **3** (blue); **4** (red) in $CHCl_3$.

Figure 4. Ensembles of low energy conformers of compounds **1 – 4**; 18- and 19-methyl groups of steroid core are depicted as balls (these faced to macrocyle are colored orange; away from macrocycle – gray).

Figure 5. Calculated lowest energy conformers for compounds **1 - 4**. Short interatomic distances favorable for hydrogen bond formation are marked by hash lines; numbers indicate distance in Angstroms.

Figure 6. Uptake and internalization of conjugates **1 – 4** by LNCaP cells (concentration of each conjugate in media was 25 μM; the numbers of curves corresponded to numbers of conjugates) .

Figure 7. Effect of galeterone on uptake and internalization of conjugates by prostate carcinoma cells: A - uptake and internalization of conjugate **3** by LNCaP cells; B - uptake and internalization of conjugates **1**, **2**, **4**, and **18** by PC-3 cells, (insert – structure of conjugate **18**).

LEGEND TO SCHEME

Scheme. *a* – *m*-Chloroperbenzoic acid, CH_2Cl_2, Δ, 8 h; *b* – $LiAlH_4$, THF, Δ, 2 h; *c* – RuO_2*H_2O, $KBrO_3$, acetone/H_2O, Δ, 20 min; *d* – DCC, DMAP, toluene/EtOH, r. t., 2.5 h; *e* – 15% H_2SO_4, THF, Δ, 20 min; *f* – Dess-Martin periodinane, CH_2Cl_2, r. t., 30 min; *g* – Oxalic acid, EtOH, Δ, 10 min; *h* – K_2CO_3, MeOH/H_2O, Δ, 40 min; *i* – $CF_3COOC_6F_5$, Et_3N, CH_2Cl_2, r. t., 2 h; *j* – Ethylene diamine, CH_2Cl_2, r. t., 2 h; *k* – 1,5-Diaminopentane, CH_2Cl_2, r. t., 2 h; *l* – DCC, CH_2Cl_2, r. t., 2 h

Figure 1

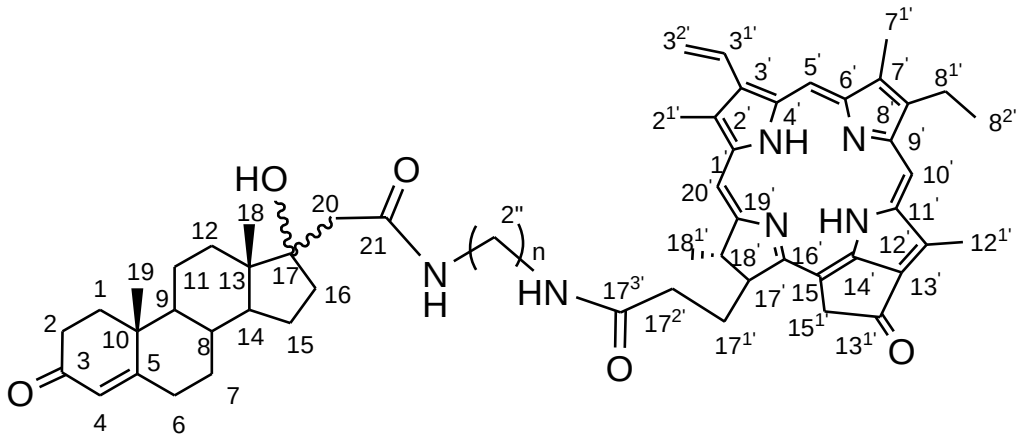

1, 17(*R*), n = 2 **3,** 17(*S*), n = 2
2, 17(*R*), n = 5 **4,** 17(*S*), n = 5

Figure 2

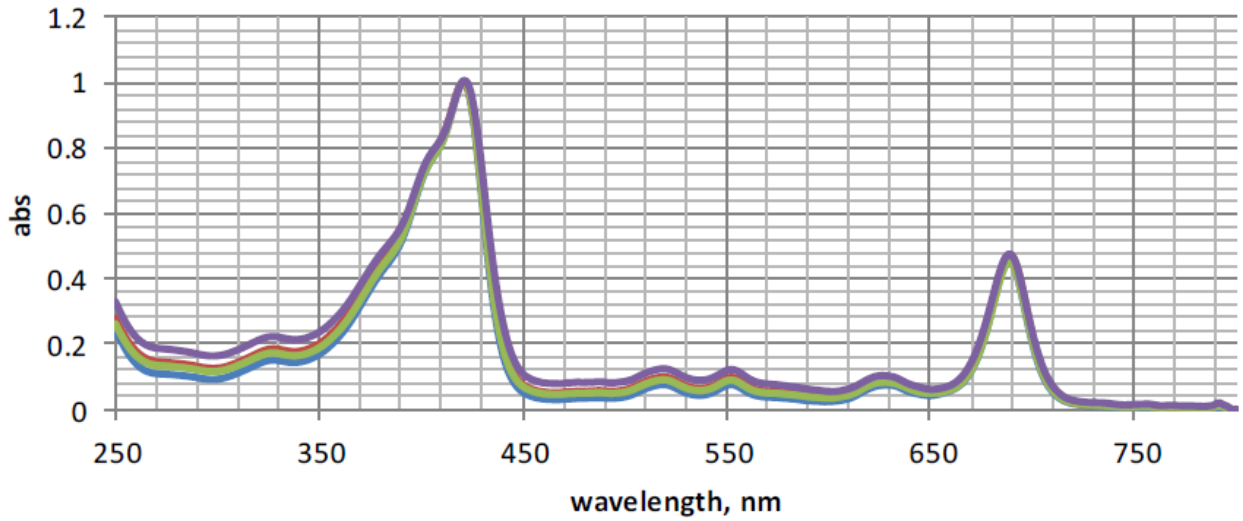

Figure 3

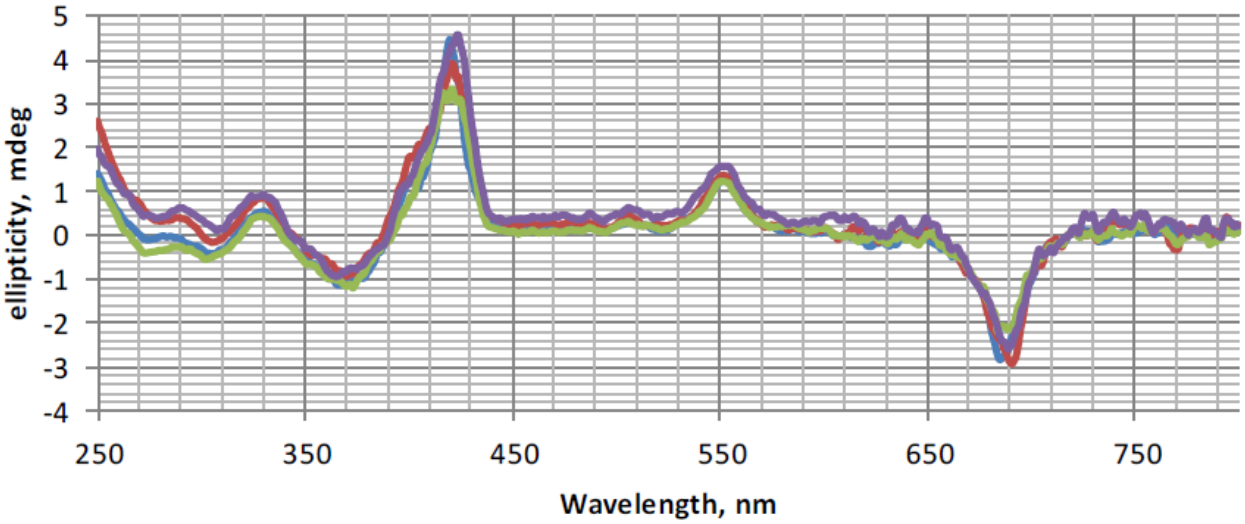
5
4
3
2
1
0
-1
-2
-3
-4
ellipticity, mdeg
250
350
450
550
650
750
Wavelength, nm

Figure 4

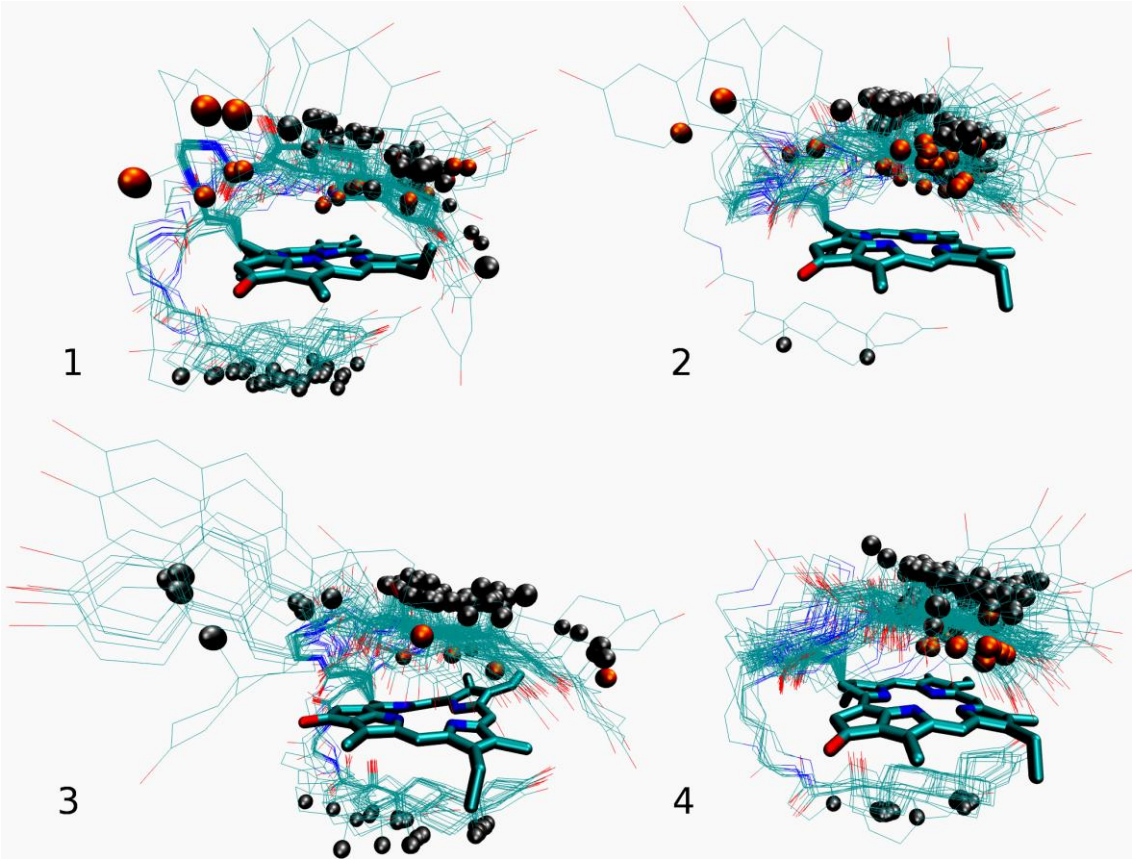

Figure 5

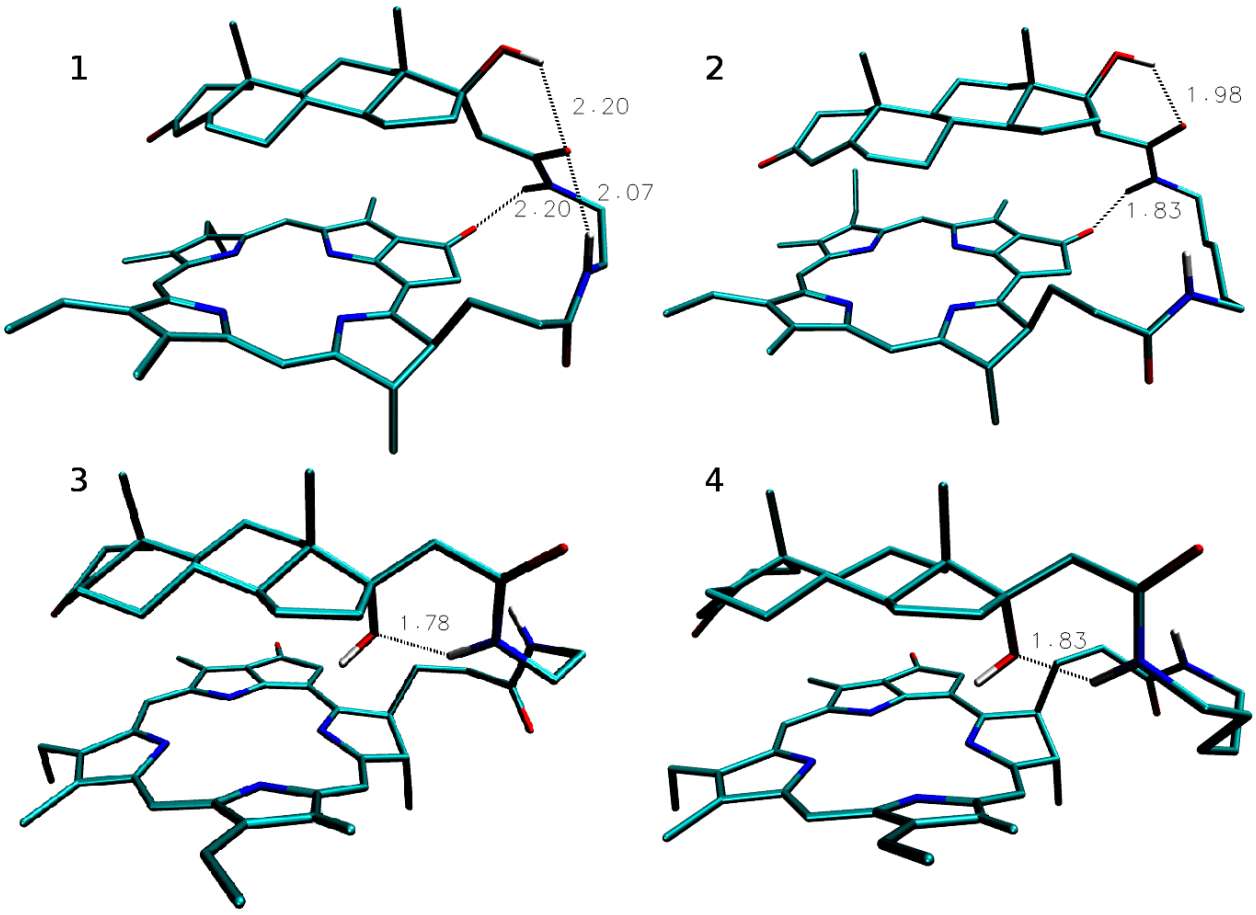

Figure 6

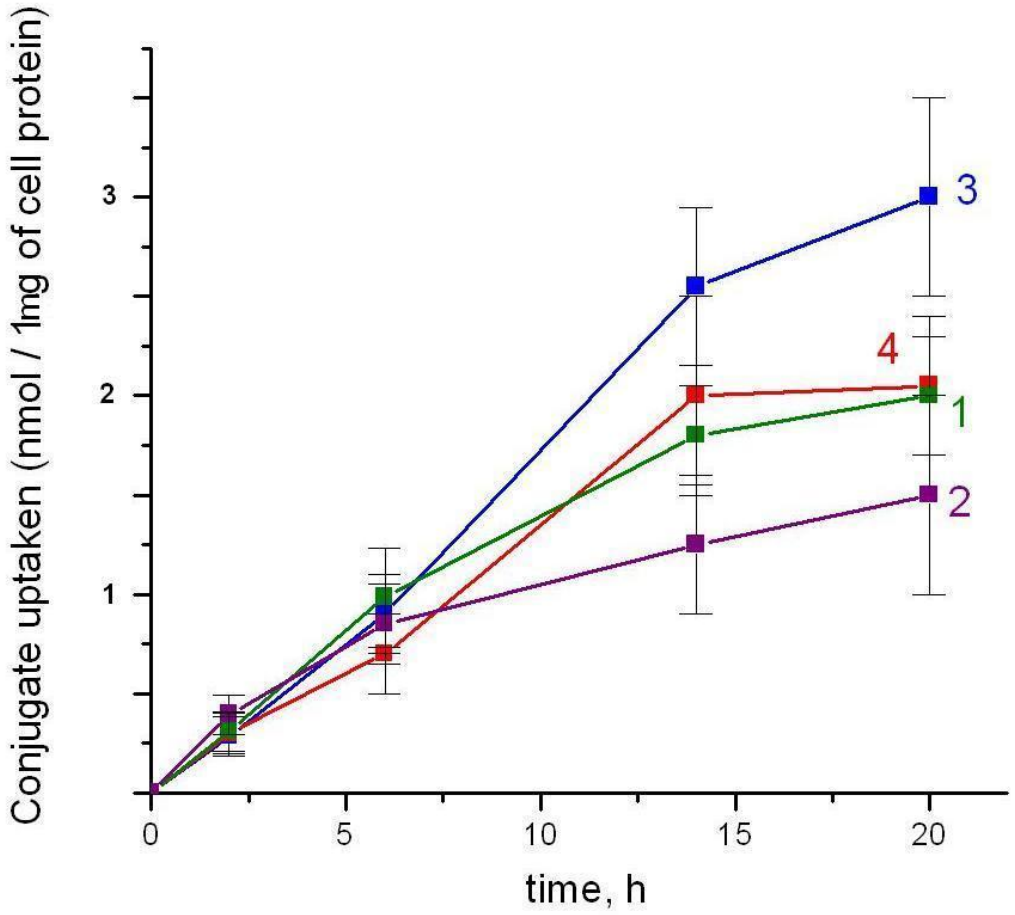
Conjugate uptaken (nmol / 1mg of cell protein)
time, h
0
5
10
15
20
1
2
3
3
4
1
2

Figure 7

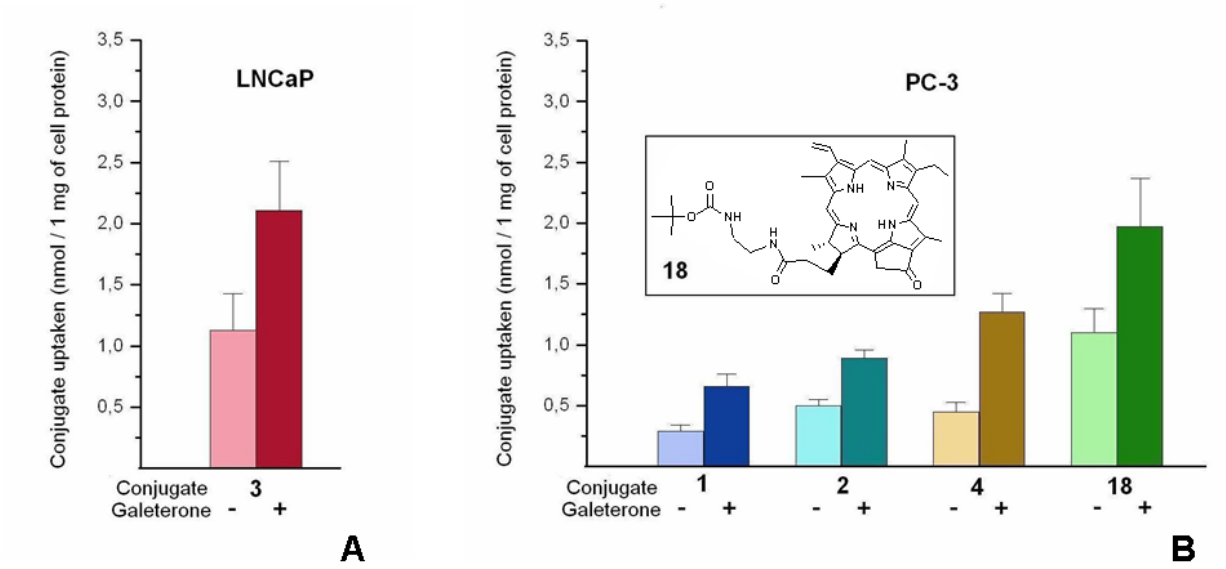
LNCaP
Conjugate uptaken (nmol / 1 mg of cell protein)
3,5
3,0
2,5
2,0
1,5
1,0
0,5
Conjugate
Galeterone
3
-
+
A
PC-3
18
1
2
4
18
B

.

Scheme 1

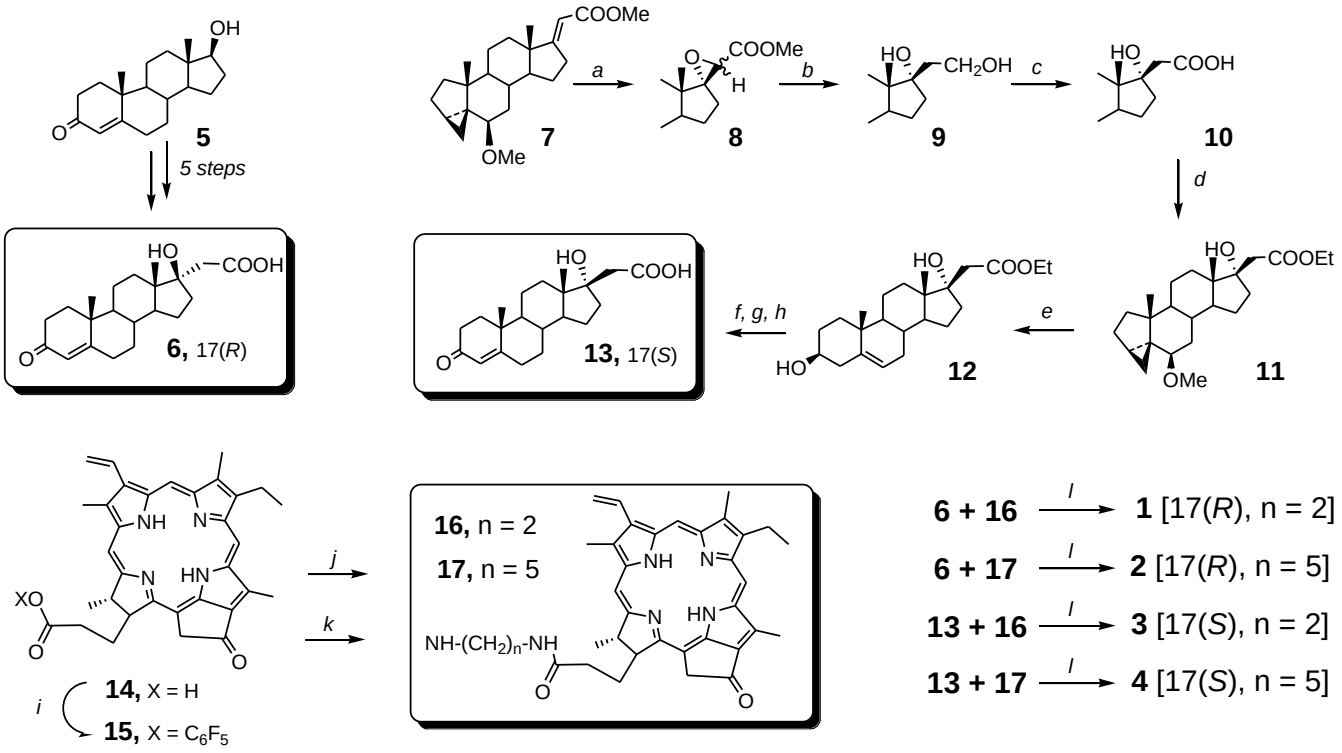
OH
O
5
5 steps
COOMe
a
7
OMe
O
COOMe
H
8
b
HO
CH2OH
9
c
HO
COOH
10
d
HO
COOEt
OMe
11
e
HO
COOEt
HO
12
f, g, h
HO
COOH
O
13, 17(S)
HO
COOH
O
6, 17(R)
NH
N
N
HN
XO
O
O
i
14, X = H
15, X = C6F5
j
k
16, n = 2
17, n = 5
NH-(CH2)n-NH
6 + 16 → 1 [17(R), n = 2]
6 + 17 → 2 [17(R), n = 5]
13 + 16 → 3 [17(S), n = 2]
13 + 17 → 4 [17(S), n = 5]
l

TABLE 1.

CHEMICAL SHIFTS (δ, ppm) OF SOME CHARACTERISTIC RESONANCES IN ^{1}H NMR SPECTRA OF CONJUGATES **1 - 4**

Compound	H-4	H-18	H-19	H-5’	H-10’	H-20’	H-1”	H-2”
1	5.56, s	0.25, s	0.75, s	9.26, s	9.04, s	8.52, s	6.61, br.t	6.30, br.t
2	5.53, s	0.73, s	1.00, s	9.31, s	9.28, s	8.51, s	6.35, br.t	5.30, br.t
3	5.53, s	0.54, s	0.88, s	9.24, s	9.10, s	8.48, s	6.78 br.t	6.24, br.t
4	5.58, s	0.25, s	0.81, s	9.32, s	9.24, s	8.50, s	6.22 br.t	5.53 br.t

TABLE 2.

EFFECTS OF CONJUGATES **1 – 4** ON VIABILITY OF LNCaP AND PC-3 CELLS (IC_{50}, μM) AT 96 h INCUBATION

Conjugate	LNCaP	PC-3
1	4.8	6.1
2	12.1	21.4
3	1.3	2.6
4	6.4	14.2